Quasi-One-Dimensional Electronic Systems Formed from Boron Dipyrromethene (BODIPY) Dyes

Raymond Ziessel,*[a] Sandra Rihn,[a] and Anthony Harriman*[b]

Abstract: Synthetic strategies have been devised that allow the rational design and isolation of highly coloured boron dipyrromethene (BODIPY) dyes that absorb across much of the visible region. Each dye has an aryl polycycle (usually pyrene or perylene) connected to the central BODIPY core through a conjugated tether at the 3,5-positions. Both mono- and difunctionalised derivatives are accessible, in certain cases containing both pyrene and perylene residues. For all new compounds, the photophysical properties have been recorded in solution at ambient temperature and in a glassy matrix at 77 K. The presence of the aryl polycycle(s) affects the absorption and emission maxima of the BODIPY nucleus, thereby confirming that these units are coupled electronically. Indeed, the band maxima and oscillator strengths depend on the conjugation length of the entire molecule, whereas there is no sign of fluorescence from the polycycle. As a consequence, the radiative rate constant tends to increase with each added appendage. The nature of the linkage (styryl, ethenyl, or ethynyl) also exerts an effect on the photophysical properties and, in particular, the absorption spectrum is perturbed in the region of the aryl polycycle. The perylene-containing BODIPY derivatives absorb over a wide spectral range and emit in the far-red region in almost quantitative yield. A notable exception to this generic behaviour is provided by the anthracenyl derivative, which exhibits charge-transfer absorption and emission spectra in weakly polar media at ambient temperature. Regular BODIPY-like behaviour is restored in a glassy matrix at 77 K. Overall, these new dyes represent an important addition to the range of strongly absorbing and emitting reagents that could be used as solar concentrators.

Keywords: dyes/pigments · energy transfer · fluorescence · sensitizers · synthesis design

Introduction

There appears to be an almost insatiable market for highly fluorescent dyes, especially for systems in which the basic fluorophore is robust, easily functionalised and resistant to triplet formation. Numerous applications, ranging from fluorescent bio-labels and sensors, to anti-forgery devices, to organo-gels and to solar concentrators, have been proposed for such materials.[1] Among the many diverse types of fluorophore in common usage, boron dipyrromethene (BODIPY) dyes have come to prominence in recent years[2] and there has been a tremendous growth in the number of publications and patents describing this class of compound.[2,3] In particular, considerable research effort has been devoted to the synthesis[4] and photophysical examination[5] of BODIPY dyes equipped with ancillary photon collectors, such as pyrene.[6] The motivation for the development of these materials stems largely from the need to enhance the (virtual) Stokes' shift,[7] thereby optimising the performance in flow cytometry and fluorescence imaging technology, and to facilitate the harvesting of a larger fraction of solar energy, thereby helping to engineer improved photon collectors.[8] A common feature of such materials is that the BODIPY nucleus and the appended light harvester, usually an aryl polycycle, remain in weak electronic communication such that each unit retains its own identity, even though intramolecular energy transfer might be extremely fast.[9] We now describe an alternative approach to the fabri-

[a] Dr. R. Ziessel, S. Rihn
Laboratoire de Chimie Moléculaire et
Spectroscopies Avancées (LCOSA)
Ecole Européenne de Chimie, Polymères et Matériaux, CNRS
25 rue Becquerel, 67087 Strasbourg Cedex 02 (France)
Fax: (+33) 368852761
E-mail: ziessel@unistra.fr
Homepage: http://www-lmspc.u-strasbg.fr/lcosa

[b] Prof. Dr. A. Harriman
Molecular Photonics Laboratory, School of Chemistry
Bedson Bldg, Newcastle University
Newcastle upon Tyne, NE1 7RU (UK)
Fax: (+44) 191-222-8660
E-mail: anthony.harriman@ncl.ac.uk

Supporting information for this article is available on the WWW under http://dx.doi.org/10.1002/chem.201001142.

cation of next-generation BODIPY dyes that absorb over much of the visible spectral range and fluoresce in the far-red region. Our strategy involves the synthesis of BODIPY dyes wherein the ancillary photon collector forms part of the overall conjugated network running throughout the dye molecule. One such series of compounds has styryl-based connections at the 3,5-positions of the dipyrromethene core,[10] which ensure excellent conjugation across the molecule. In seeking to extend and generalise this work, two additional series of compounds having the polycycle attached to the dipyrromethene nucleus through a vinyl or an acetylene linkage have also been prepared. Finally, we report a notable exception to the generic principle of increased π-conjugation for the BODIPY family of dyes.

A question might be raised at this point as to how to establish the difference between (1) rapid intramolecular electronic energy transfer (EET) from the appended polycycle to the BODIPY dye and (2) internal conversion between singlet-excited states resident on the same giant molecule. In this respect, it should be noted that sub-ps EET has already been reported[11] for several closely linked BODIPY–anthracene dyads, and the rates were rationalised in terms of mutual orientation factors. One key point to bear in mind is that to properly examine intramolecular EET in extended π-systems, it is necessary that the presence of the substituent does not perturb the molecular orbital, or transition dipole moment vector, of the BODIPY dye. In the event of strong electronic coupling persisting, it is important to consider internal conversion between coupled electronic states of the same system. For the dyes described here, the latter case seems to dominate.

Results and Discussion

Synthesis and characterisation: The target compound comprising fused BODIPY (B), perylene (Pe) and pyrene (Py) residues, hereafter abbreviated as PeBPy, could be routinely prepared as illustrated in Scheme 1. To aid interpretation of the photophysical properties, related compounds were also prepared and fully characterised as also shown in Scheme 1. The relatively insoluble starting material B_1, containing one iodo and two bromo residues, requires selective functionalisation at the most reactive site (i.e., the iodo group) to impart solubility and polarity to facilitate the purification procedure. Cross-coupling of ethyl 6-heptynoate with precursor B_1 provided B in 78% yield. The selectivity was checked by NMR spectroscopy, while EI-MS provided clear evidence for a molecular peak with an isotopic profile corresponding to B (see the Supporting Information). We next examined the connection of 3-ethynylperylene[12] using classical Pd^0-promoted cross-coupling reactions. The use of one equivalent of 3-ethynylperylene gave a mixture of two compounds, PeB and Pe_2B, which could be separated and were isolated in yields of 42% and 39%, respectively. Notably, the symmetrical model compounds, Pe_2B and Py_2B, could be produced in high yields (>85%) under similar conditions
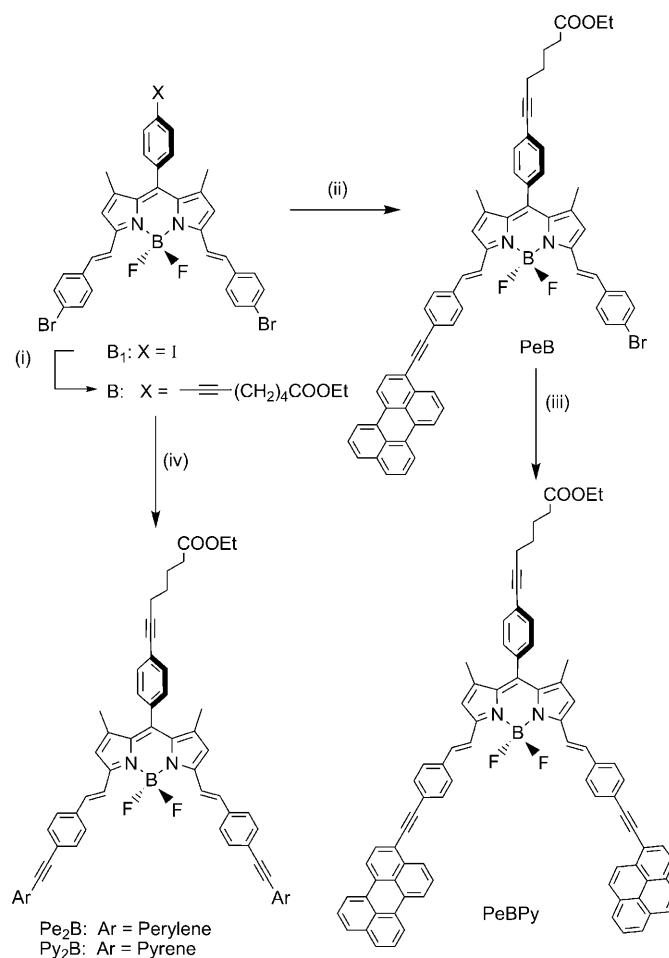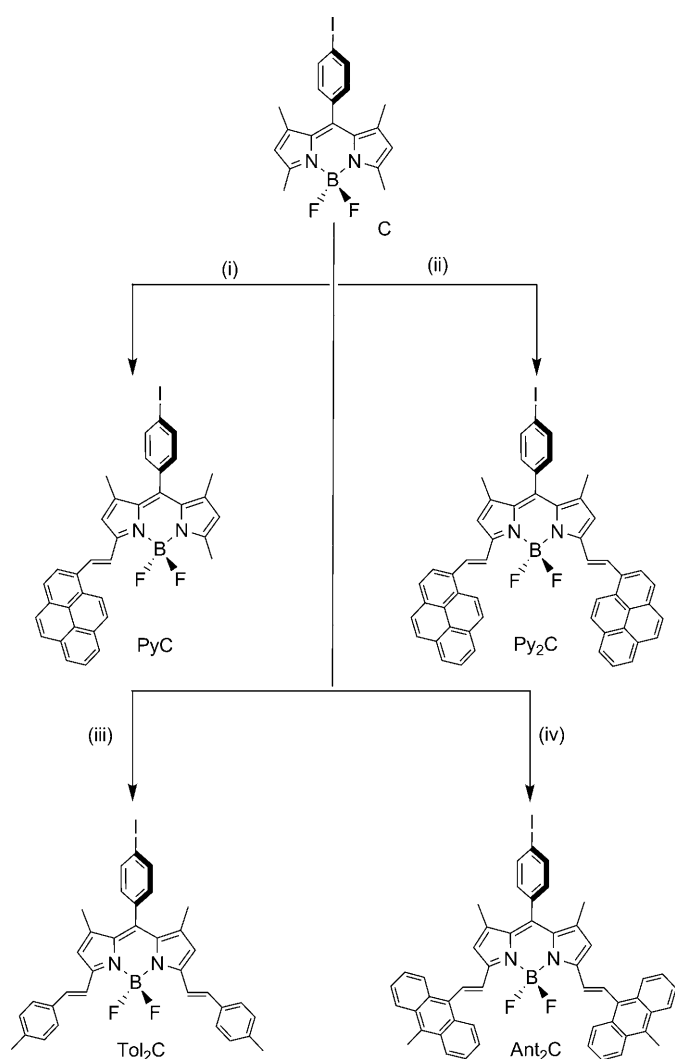

Scheme 1. Key: (i) HC≡C(CH$_2$)$_4$COOEt (1.5 equiv), benzene/THF (20:1), diisopropylamine, [Pd(PPh$_3$)$_2$Cl$_2$] (6 mol%), CuI (10 mol%), RT, 2 days; (ii) 3-ethynylperylene (1 equiv), THF, diisopropylamine, [Pd(PPh$_3$)$_4$] (6 mol%), 60°C, 12 h; (iii) 1-ethynylpyrene (1 equiv), THF, diisopropylamine, [Pd(PPh$_3$)$_4$] (6 mol%), 60°C, 10 h; (iv) 3-ethynylperylene (2.2 equiv) or 1-ethynylpyrene (2.2 equiv), THF, diisopropylamine, [Pd-(PPh$_3$)$_4$] (6 mol%), 60°C, 18 h.

but using the ethynyl derivatives in excess. The final coupling reaction involved attachment of a 1-ethynylpyrene[13] residue to the pre-organised PeB dye (Scheme 1).

The chemical structures and molecular compositions of these new green dyes have been unambiguously assigned on the basis of NMR spectroscopy, mass spectrometry and elemental analyses. The well-defined ^{1}H NMR spectra exclude the presence of aggregates. Interestingly, grafting a perylene moiety onto B leading to PeB provides a characteristic deshielded doublet at $\delta = 8.32$ ppm and two β-pyrrolic proton signals at $\delta = 6.63$ and 6.85 ppm.[9a] Subsequent attachment of the pyrene unit introduces an additional doublet at $\delta = 8.75$ ppm, while two singlets at $\delta = 6.70$ and 6.92 ppm are still present. Such behaviour is indicative of a strong electronic interaction between the aryl residues and the dipyrromethene core.[9b] For the symmetrically substituted Pe_2B and Py_2B dyes, only one doublet is observed, this appearing at $\delta = 8.35$ ppm for Pe and at $\delta = 8.72$ ppm for Py. In each case,

a singlet is observed for the β-pyrrolic protons at $\delta = 6.75$ and 6.98 ppm, respectively. The characteristic H,H coupling constant of 16.3 Hz is diagnostic of an *E* conformation of the double bonds,[14] which remains unchanged during subsequent chemical transformations. Note that ^{13}C NMR spectroscopy can be used to follow the build up of the ethynylene connections because of the highly characteristic signals seen in the range $\delta = 80$–100 ppm.
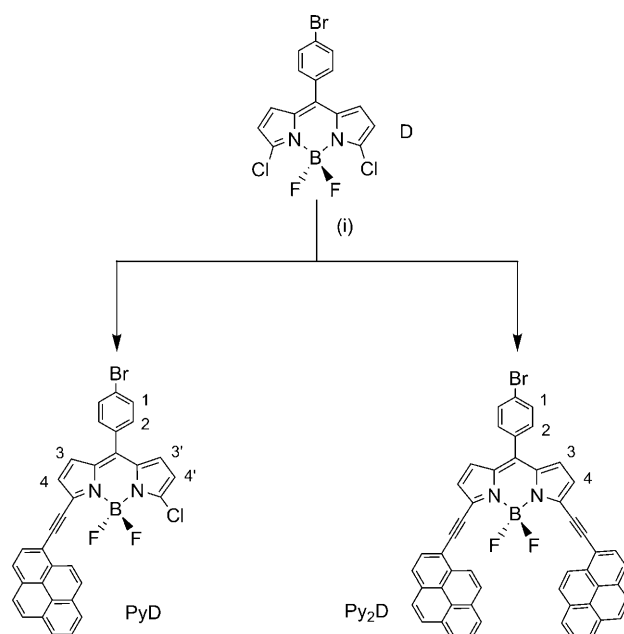
In an effort to expand this series of fused BODIPY dyes, we set out to eliminate the ethynylphenyl linkage as a means of decreasing the degree of conformational heterogeneity (Scheme 2). Thus, a Knoevenagel reaction[15] was used to condense C with 1-pyrenecarboxaldehyde. The use of various BODIPY/pyrene ratios permitted forcing the reaction in favour of either the mono- or disubstituted compounds PyC or Py$_2$C, respectively. The poor solubility of Py$_2$C facili-

tated its separation from PyC, which could then be purified by column chromatography. A similar synthetic procedure was used to produce the reference tolyl derivative Tol$_2$C and the anthracenyl compound Ant$_2$C (Scheme 2). In the latter cases, preparation of the monosubstituted derivatives proved to be very difficult because of their similar solubilities and polarities to those of the disubstituted compounds.

Having omitted the ethynylphenyl relay, it was of interest to compare the coupling properties of ethene and ethyne linkages. This was done by reference to the pyrene-containing derivatives. To reach this goal without modifying the BODIPY skeleton, we tried first to convert the ethenyl PyC and Py$_2$C derivatives into the ethynyl-linked compounds by addition of Br$_2$ to the double bonds, followed by elimination of HBr under basic conditions. Despite varying the experimental conditions (solvent, temperature, microwave irradiation, etc.), these experiments failed to give viable quantities of the desired compounds. Alternatively, we employed a recently developed protocol that enabled us to produce the dichloro-substituted BODIPY D (Scheme 3).[16,17] It has been

Scheme 2. Key: (i) 1-pyrenecarboxaldehyde (1 equiv), toluene, piperidine, *p*-TsOH trace, reflux, Dean–Stark; (ii) 1-pyrenecarboxaldehyde (2.5 equiv), toluene, piperidine, *p*-TsOH trace, reflux, Dean–Stark; (iii) 4-toluenecarboxyaldehyde (3 equiv), toluene, piperidine, *p*-TsOH trace, reflux, Dean–Stark; (iv) 10-methylanthracene-9-carboxaldehyde (3.5 equiv), toluene, piperidine, *p*-TsOH trace, reflux, Dean–Stark.

Scheme 3. Key: (i) 1-ethynylpyrene (1 equiv), THF, triethylamine, [Pd-(PPh$_3$)$_2$Cl$_2$] (10 mol%), CuI (12 mol%), RT, about 6 h.

established previously that replacement of both chloro groups by alkynyl functions can be brought about in the presence of palladium(0) catalysts.[17,18] In this specific case, the phenyliodo moieties in the BODIPY series B and C had to be replaced by the less reactive phenylbromo group, and the two methyl groups in the 1,7-positions had to be omitted to avoid steric crowding. After some trials, the mono- and disubstituted alkynylpyrene derivatives PyD and Py$_2$D were isolated from D as starting material.

For the new vinyl-based molecules, the number of resonances corresponding to the β-pyrrolic protons (labelled 4

and 4′) is diagnostic of the level of substitution (i.e., mono- versus di-). For the former species, two doublets of an AB pattern are found in the range $\delta = 6.95$ to 6.90 ppm, whereas a typically narrow AB system is found in the disubstituted case; this situation holds true for PyC, Py$_2$C, Tol$_2$C and Ant$_2$C. In each of the vinyl-based molecules, the observed 16 Hz proton–proton coupling constant is in keeping with an E conformation of the double bonds,[14] a situation consistent with the type of condensation reaction used.[15] For both PyD and Py$_2$D, the degeneracy of the AB quartet arising from the β- and γ-pyrrolic protons (labelled 3 and 3′) is diagnostic of the degree of substitution. For the monosubstituted PyD, two AB quartets are seen, with that at $\delta = 6.7$ ppm having a relatively large coupling constant of 44 Hz and being representative of the chloro-substituted ring, and the second, narrow AB quartet seen at $\delta = 6.9$ ppm corresponding to the alkyne-substituted pyrrole site. It is also informative to note the deshielding of the proton in the α-position of the pyrene residue caused by its proximity to the alkyne tether; its integration further confirmed the degree of substitution of the BODIPY nucleus (Figure 1).

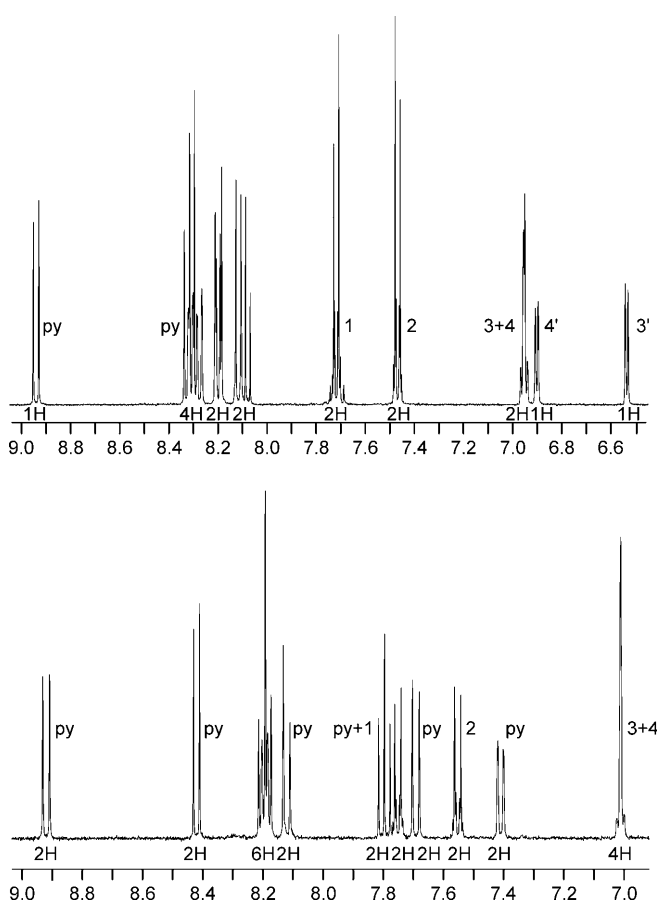**Photophysics of the styryl derivatives B**: Absorption spectra recorded for the various fused dyes in methyltetrahydrofu-ran (MTHF) solution at room temperature show a rich mixture of transitions across the visible and near-UV regions (Figure 2). In each case, optical transitions associated with
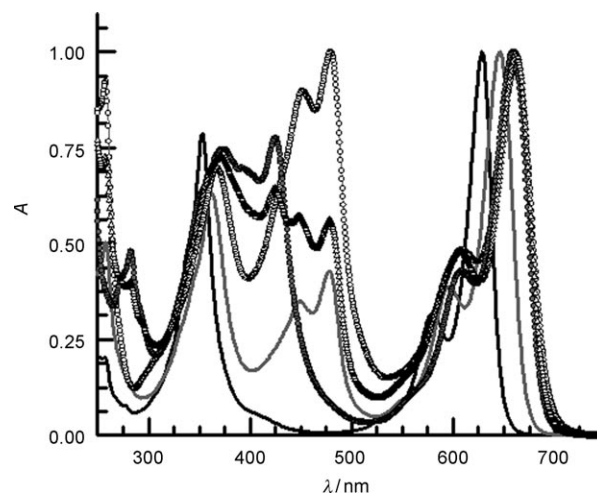

Figure 2. Absorption spectra recorded for the various styryl BODIPY dyes in MTHF at room temperature: B (black), PeB (grey), Pe$_2$B (open circles), Py$_2$B (solid dots) and PeBPy (open triangles).

the BODIPY nucleus can be recognised in the far-red region of the spectrum.[19] Typically, these transitions appear as a set of overlapping bands with a pronounced 0,0 peak (λ_{ABS}) in the region 640–685 nm (Table 1). Notably, the acetylenic function attached through the central *meso* position has no effect on the position or strength of this transition. However, the nature and number of polycycles fitted to the styryl residues has a strong influence on the position of the 0,0 peak ($\nu_{0,0}$) and on the half-width ($\Delta\nu_{1/2}$) of the individual bands that comprise the relevant absorption envelope (Table 2); these values have been derived by fitting the entire absorption transition to a series of Gaussian compo-

Figure 1. Typical proton NMR spectra (400 MHz) for PyD (top) and Py$_2$D (bottom) in [D$_2$]dichloromethane at RT. For proton labelling, see Scheme 3; py refers to the pyrene protons.

Table 1. Photophysical properties recorded for the styryl-bridged dyes in MTHF at room temperature.

Cmpd	λ_{ABS} [nm]	ε_{MAX} [M^{-1}cm^{-1}][a]	λ_{FLU} [nm][b]	SS [cm^{-1}]	Φ_F[c]	τ_S [ns][d]	k_{RAD}/ 10^{8}[e,f]
B	629, 579	81375 (0.41)	641	300	0.75	4.5	1.65 (1.15)
PeB	646, 596	110630 (0.67)	664	420	0.76	4.1	1.85 (1.75)
Pe$_2$B	661, 610	128450 (1.08)	683	465	0.86	3.6	2.40 (2.60)
Py$_2$B	659, 608	121200 (0.82)	675	360	0.80	3.9	2.05 (2.05)
PeBPy	662, 606	124400 (0.97)	680	400	0.83	3.75	2.20 (2.15)

[a] Molar absorption coefficient for the lowest-energy absorption band with the corresponding oscillator strength given in parentheses. [b] Independent of excitation wavelength. [c] Direct excitation into the BODIPY absorption transition at 590 nm. [d] Excitation at 410, 470 and/or 590 nm. [e] Radiative rate constant given in units of s^{-1}. [f] Given in parentheses is the radiative rate constant calculated from the Strickler–Berg expression.

Table 2. Parameters derived from spectral curve-fitting of room temperature data.

Cmpd	$\nu_{0,0}$ [cm^{-1}]	$\Delta\nu_{1/2}$ [cm^{-1}][a]	ν_{FLU} [cm^{-1}]	$\Delta\nu_{1/2}$ [cm^{-1}][b]	S_Δ	$h\omega_M$ [cm^{-1}]	$h\omega_L$ [cm^{-1}]
B	15598	540	15605	530	0.35	1335	495
PeB	15440	630	15050	575	0.38	1365	575
Pe$_2$B	15065	755	14450	700	0.36	1360	680
Py$_2$B	15120	675	14805	660	0.35	1345	645
PeBPy	15090	700	14705	700	0.36	1365	670

[a] Half-width of fitted absorption band. [b] Half-width of fitted fluorescence band.

nents. This analysis indicates that the absorption transition is coupled to an averaged low-frequency torsional mode that increases systematically with increasing molecular size; for example, this term increases from 456 cm^{-1} for B to 596 cm^{-1} for Pe$_2$B. As the total number of peripheral double bonds increases, there is a progressive shift of $\nu_{0,0}$ towards lower energy and a substantial increase in $\Delta\nu_{1/2}$ (Figure 3,
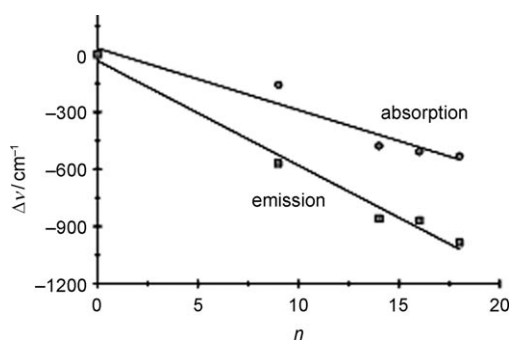

Figure 3. Effect of the change in the number of peripheral double bonds (n) on the magnitude of the spectral shifts for the 0,0 transitions for both absorption and emission spectra recorded in MTHF at room temperature.

Table 2); note that each pyrene and perylene residue contributes seven and nine additional peripheral double bonds, respectively, to the π-conjugated network. The basic BODIPY core also displays a strong absorption band over the 350–450 nm range that seems to be due to a combination of two or more transitions. Interestingly, the sharp absorption transition seen at around 360 nm, attributable to the S$_0$–S$_3$ transition of the BODIPY nucleus, also shifts progressively towards lower energy as the size of the substituent is increased. The corresponding S$_0$–S$_2$ absorption transition, seen as a weak shoulder at about 420 nm, becomes obscured by the more intense π,π* transitions due to the aromatic polycycle.

The perylene unit present in both PeB and Pe$_2$B displays strong absorption bands at around 450 and 470 nm, together with a transition localised at around 360 nm. These two absorption envelopes are little affected by the number of perylene units present or by the replacement of one perylene with pyrene. Nonetheless, the bands are red-shifted and broadened significantly with respect to those of 1-ethynyl-

perylene, showing that the appended BODIPY core influences the electronic properties of the perylene chromophore. The same conclusion is reached for the Py residue. Thus, π,π* transitions localised on the Py unit are evident as a series of bands extending between 370 and 450 nm that remains unaffected by replacing one pyrene with perylene. This absorption envelope is markedly different from that found for 1-ethynylpyrene and also for the molecular dyad formed by replacing the fluorine atoms with 1-ethynylpyrene residues.[20] Again, the conclusion is that the polycycle and BODIPY nucleus are in strong electronic contact.

This impression is strengthened by consideration of the molar absorption coefficients (ε_{MAX}) determined for the BODIPY-based transition located at long wavelengths (Table 1). The magnitude of ε_{MAX} evolves steadily with increasing molecular length. There is a more pronounced increase in the corresponding oscillator strength (f) for this transition, caused by the increased half-widths and ε_{MAX} values. Indeed, f increases from 0.41 for B to 1.08 for the most extended system, Pe$_2$B (Table 1). This is clear evidence for electronic coupling between the aryl polycycle and the BODIPY core.

Fluorescence is readily observed from these dyes (Figure 4) and, in each case, the 0,0 transition (λ_{FLU}) occurs at slightly lower energy than that of the corresponding absorption transition. Stokes' shifts (SS) tend to be rather small (Table 1),[21] indicating that the geometry does not change significantly upon excitation. Furthermore, the change in emission maximum tracks the shifts noted for the absorption band and λ_{FLU} moves progressively towards lower energy on increasing the effective size of the ancillary photon collector (Figures 3 and 4). The effect on the emission maximum is more pronounced, by a factor of about 50%, than that seen for the corresponding absorption band, indicating that electronic coupling is stronger for the excited state manifold than for the corresponding ground state. Additional changes are seen for the fluorescence quantum
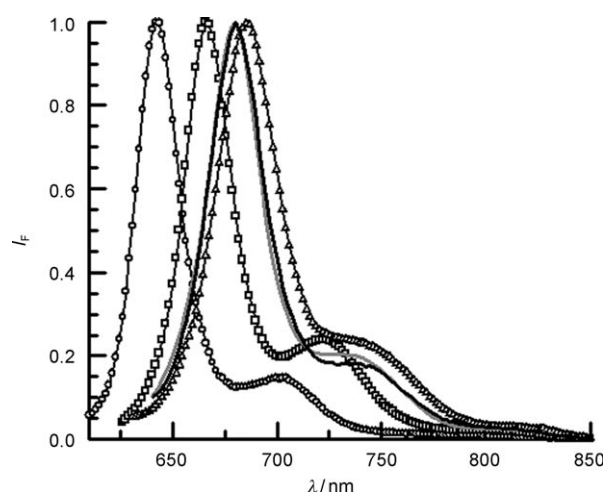

Figure 4. Fluorescence spectra recorded for the various fused BODIPY dyes in MTHF at room temperature: B (○), PeB (□), Pe$_2$B (black), Py$_2$B (grey) and PeBPy (△).

FULL PAPER

yields (Φ_F), which tend to increase as the emission maximum moves towards lower energy, and for the fluorescence lifetimes (τ_S), which follow the opposite general trend (Table 1). For each compound, there is reasonably good mirror symmetry between the fluorescence and (lowest-energy) absorption spectral patterns and the excitation spectra match well with the absorption spectra over the entire wavelength range. This latter observation is consistent with all absorbed photons being channelled to the emissive state. The radiative rate constants (k_{RAD})[22] increase as the emission maximum moves towards lower energy and remain in excellent agreement with the corresponding value calculated from the Strickler–Berg expression.[23] The increase in k_{RAD} can be traced to the effect of the substituent on the oscillator strength. As a result, the anticipated fall in k_{RAD} as the mean emission wavenumber decreases is offset by the increased oscillator strength and Φ_F tends to increase as the series evolves. Again, this finding points clearly to coupling between the termini and the central BODIPY core. It is also notable that the rate constants ($k_{NR} = (1-\Phi_F)/\tau_S$)) for nonradiative decay of the BODIPY-based excited singlet state tend to decrease with increasing size of the substituent, in apparent contradiction to the energy-gap law.[24] We will return to this point later.

Spectral deconvolution of the total emission envelope recorded for B implies a minimum of six Gaussian-shaped components, sharing a common half-width of around 530 cm^{-1}. This analysis further indicates that both medium- ($h\omega_M = 1335$ cm^{-1}) and low-frequency ($h\omega_L = 495$ cm^{-1}) vibrational modes are coupled to nonradiative decay of the lowest-energy singlet-excited state at room temperature (Table 2). The monoperylene derivative, PeB, exhibits a somewhat broader emission profile, but retains both medium- and low-frequency modes; it is notable that comparable half-widths are found for the absorption and emission spectral profiles for each dye. Spectral broadening, as measured in terms of the derived $\Delta\nu_{1/2}$ term, increases as the overall size of the substituent increases, but $h\omega_M$ tends to remain fairly constant at around 1360 cm^{-1}. This latter value may be suggestive of a C=C bending vibration being coupled to nonradiative decay. Interestingly, the coupled $h\omega_L$ parameter increases with increasing bulk of the substituent but, throughout the series, is notably higher than that derived from the absorption transition. This vibronic mode is most likely associated with torsional motion of the styryl linkage(s), with the magnitude increasing with increasing electron delocalisation.[25] In contrast, the Huang–Rhys factor[26] (S_Δ) is insensitive to the size of the appendage (Table 2). This latter finding suggests to us that S_Δ is essentially determined by the nature of the connection at the BODIPY unit and this feature does not change throughout the series. In molecular spectroscopy, the Franck–Condon overlap factors establish the probability of particular electronic-vibronic transitions and S_Δ gives a quantitative appreciation of the strength of this interaction.[25] An S_Δ value of less than 0.1 can be considered as representing weak elec-

tronic-vibronic coupling, whereas a value exceeding unity is taken to indicate strong coupling.

The low-energy region of the absorption spectrum recorded for B in MTHF shows fine structure due to a combination of low- ($h\omega_L = 456$ cm^{-1}) and medium-frequency ($h\omega_M = 1430$ cm^{-1}) vibrational modes. Similar patterns are seen in the fluorescence and excitation spectra, suggesting that the absorption spectral envelope is due to a single transition. Stepwise cooling of B in MTHF leads to a progressive red shift of both the absorption and emission maxima, with the Stokes' shift decreasing steadily as the temperature is lowered until reaching the glassy matrix, for which SS = 190 cm^{-1}. The emission band half-width ($\Delta\nu_{1/2}$) decreases noticeably upon cooling, especially between 295 and 200 K, and reaches a value of 270 cm^{-1} at 77 K. The red shifts can be explained in terms of structural distortions being dampened at low temperature, such that there is an extension of the conjugation length. Spectral analysis of the low-temperature data shows that $h\omega_M$ splits into two modes of 1450 and 1200 cm^{-1}, whereas $h\omega_L$ appears as a progression of low-frequency modes of about 310 cm^{-1}. Thermal fluctuations at higher temperatures lead to the observed broadening of the spectral bands.[27] It is noticeable that the excitation spectra show identical effects.

The same type of temperature-dependent spectral analysis was applied to the functionalised compounds in MTHF. Essentially similar behaviour was observed in each case, although the band half-widths remain larger for the derivatives than for B and, even at 77 K, the spectra were not so well resolved. This situation is illustrated for Pe$_2$B in Figure 5. Thus, the emission band half-width observed at 77 K is 520 cm^{-1}, whereas the coupled $h\omega_L$ has a value of 460 cm^{-1}, both parameters being significantly larger than those determined for B. Furthermore, $h\omega_M$ splits into separate vibronic modes of 980 and 1345 cm^{-1} at lower temperatures, at which thermal broadening is greatly diminished. These refined values support the conclusions drawn from analysis of the room temperature spectra.
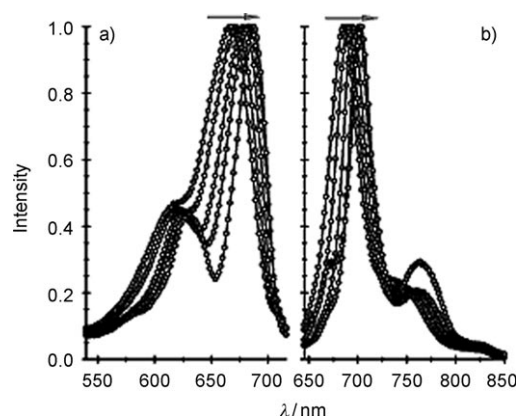

Figure 5. Effect of decreasing temperature on the a) excitation and b) fluorescence spectra recorded for Pe$_2$B in MTHF: temperatures 295, 245, 195, 145 and 95 K.

Despite strenuous efforts, we were unable to resolve fluorescence from the polycyclic appendage, although the isolated polycycle itself is strongly emissive. Indeed, the maximum Φ_F value for the Pe and Py units in the various multicomponent dyes was estimated to be $< 10^{-5}$, while the corresponding τ_S values must be < 30 ps. Interrogation of Pe_2B in MTHF by ultrafast transient spectroscopy following direct excitation of the Pe unit showed the first excited singlet state on the BODIPY dye to be formed within 300 fs. This is significantly faster than previously found for related dyes in which the subunits are interconnected either through the boron atom or at the *meso* position.[6] Such behaviour could result from very fast intramolecular energy transfer, assuming that the Pe unit forms a discrete excited state that is decoupled from the BODIPY manifold, or by way of fast internal conversion, in the event that the molecule functions as a single chromophore.

Photophysics of the ethenylene derivatives C: Further studies were carried out to assess the contribution made by the connecting benzene ring. Firstly, it was noted that the terminal iodine atoms present in series C have no effect on the photophysical properties since those recorded for Tol_2C were essentially the same as those recorded for compound B (Table 3). More significantly, marked blue shifts were observed for both the absorption and fluorescence maxima recorded for the monoethenyl derivative PyC, which can be attributed to the shortened conjugation pathway. Increasing the extent of π conjugation causes a significant red shift in both the absorption and emission maxima and elevates the molar absorption coefficient (and related oscillator strength). The S_0–S_2 transitions found for both B and Tol_2C appear as weak, broad absorption bands with maxima at around 400 nm. There is an additional absorption transition, S_0–S_3, at 360 nm that appears as a narrow band. Notably, the

intensity of this latter band is reduced by a factor of about three for Tol_2C relative to B. For PyC and Py_2C, high-energy absorption transitions appear at 395 and 430 nm, respectively, which may contain a contribution from the pyrene chromophore. Excitation spectra match absorption spectral profiles recorded across the window from 250 to 700 nm. As above, it was not possible to observe fluorescence that could be attributed to the pyrene residue for either PyC or Py_2C.

As noted above, Φ_F remains high for these ethenylene-based compounds and tends to increase with increasing extent of π conjugation (Table 3). The radiative rate constants, being in good accord with those calculated from the Strickler–Berg expression,[23] show a similar increase along the series, but the excited-state lifetimes decrease as the emission maximum shifts towards lower energy. This generic behaviour is comparable to that described above.

Spectral curve-fitting routines were carried out as described earlier to ascertain the properties that are characteristic of these ethenylene-linked derivatives, and the results are collected in Table 4. As expected, Tol_2C closely resem-

Table 4. Parameters derived from spectral curve-fitting of room temperature data.

Cmpd	$\nu_{0,0}$ [cm^{-1}]	$\Delta\nu_{1/2}$ [cm^{-1}][a]	ν_{FLU} [cm^{-1}]	$\Delta\nu_{1/2}$ [cm^{-1}][b]	S_Δ	$\hbar\omega_M$ [cm^{-1}]	$\hbar\omega_L$ [cm^{-1}]
PyC	16765	550	16195	630	0.46	1320	580
Tol_2C	15800	610	15495	585	0.31	1300	615
Py_2C	14485	740	13870	620	0.33	1340	805
Ant_2C	15630	1855	14695	785	0.69	NA	680
PyD	16390	1180	15245	1265	0.39	1275	700
Py_2D	14425	1005	13810	745	0.53	1350	575

[a] Half-width of fitted absorption band. [b] Half-width of fitted fluorescence band.

bles B and there are no notable differences between these two derivatives. The monopyrene analogue, PyC, shows the highest S factor and requires inclusion of both medium- and low-frequency vibronic terms, the latter being the lowest of all the coupled vibrational modes extracted from the spectral fits. Upon extending the degree of π conjugation by moving to Py_2C, there is a pronounced decrease in S and an increase in $\hbar\omega_L$. The generic trend seems to agree with that derived for the B series, such that the bridging ethynylbenzene residue has little direct effect on the photophysical properties of the dye. In particular, there is no great change in the band half-widths and this is interpreted in terms of the internal flexibility remaining similar for the two sets of compounds.

To probe this latter effect in more detail, the emission spectra were recorded in an MTHF glass at 77 K. In each case, the band maximum undergoes a pronounced red shift and narrowing on cooling. For example, λ_{FLU} moves to 738 nm for Py_2C, while the band half-width decreases to 330 cm^{-1} (Figure 6). The magnitude of the red shift is more exaggerated than that found for Py_2B (i.e., 315 cm^{-1} compared with 230 cm^{-1}), whereas the relative decrease in the

Table 3. Photophysical properties recorded for the ethenylene- and ethynylene-bridged dyes in MTHF at room temperature.

Cmpd	λ_{ABS} [nm]	ε_{MAX} [M^{-1}cm^{-1}][a]	λ_{FLU} [nm][b]	SS [cm^{-1}]	Φ_F[c]	τ_S [ns][d]	k_{RAD}/ 10^{8}[e,f]
PyC	598	93600 (0.62)	618	540	0.64	4.0	1.60 (1.65)
Tol_2C	631	101200 (0.76)	645	345	0.75	4.05	1.85 (2.00)
Py_2C	691	121700 (1.05)	720	645	0.80	3.6	2.20 (2.30)
Ant_2C	632	123400 (1.13)	714	935	0.038	0.35	1.10
PyD	609	83200 (0.69)	664	1360	0.34	2.1	1.60 (1.65)
Py_2D	692	99500 (0.76)	727	660	0.54	3.0	1.80 (1.75)

[a] Molar absorption coefficient for the lowest-energy absorption band with the corresponding oscillator strength given in parentheses. [b] Independent of excitation wavelength. [c] Direct excitation into the BODIPY absorption transition at 590 nm. [d] Excitation at 410, 470 and/or 590 nm. [e] Radiative rate constant given in units of s^{-1}. [f] Given in parentheses is the radiative rate constant calculated from the Strickler–Berg expression.
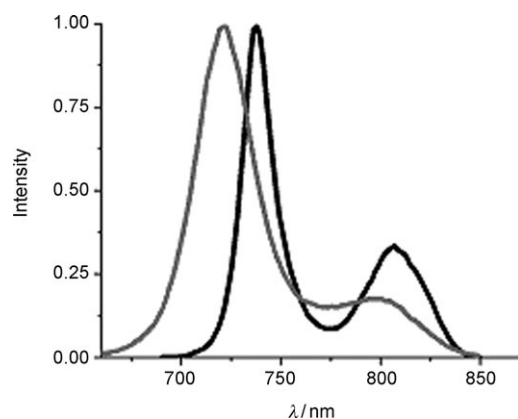
Figure 6. Fluorescence spectra recorded for PyC in MTHF at room temperature (grey curve) and 77 K (black curve).

half-width remains comparable. As noted above, the medium-frequency vibration coupled to the excited-state decay for the C-series is split at 77 K. Thus, for Py_2C at 77 K we find that $h\omega_M$ appears as a pair of vibrations with individual values of 1100 and 1350 cm^{-1}. Under the same conditions, $h\omega_L$ takes on a value of 350 cm^{-1}. For all three ethenylene derivatives, there is a small but significant increase in the magnitude of S_Δ on cooling to 77 K, with the derived values being 0.55, 0.33 and 0.39 for PyC, Tol$_2$C and Py$_2$C, respectively. These perturbed S_Δ factors are a consequence of the reduced $h\omega_L$ values, which themselves are taken to reflect an increase in the degree of π conjugation due to planarisation of the molecule at low temperatures.[28] For Py$_2$B at 77 K, the S_Δ factor is 0.36 compared to a room temperature value of 0.34, such that the geometry of this compound is little affected by cooling.

Photophysics of the ethynylene derivatives D: To further explore the effects of conformational disorder on fused BODIPY dyes, a few compounds were prepared in which an ethynylene linkage replaced the ethenylene group used for the other derivatives. Before making any critical comparisons, it should be noted that the monopyrene derivative PyD has a chlorine atom at the 5-position and this might affect the photophysical properties by virtue of the heavy-atom effect[29] and/or electronic factors. Indeed, it is notable that both the absorption and fluorescence bands are relatively broad, whereas Φ_F is somewhat lower than might be expected (Tables 3 and 4). The key comparator, therefore, is the bis-pyrene analogue Py$_2$D and we have examined the properties of this compound with respect to those of Py$_2$B and Py$_2$C. Absorption and emission spectra were recorded in MTHF at room temperature and the relevant data are collected in Tables 3 and 4. For Py$_2$D, the oscillator strength is modest, whereas the pyrene-based absorption transitions are clearly visible in the near-UV region. The lowest-energy absorption band, this being associated with the BODIPY chromophore, appears at 692 nm, which is considerably red-shifted with respect to all other spectra reported here; it represents a red shift of some 80 nm relative to the corre-

sponding bis-ethynyl derivative described by Boens et al.[19] This latter point is clear indication that the electronic levels of BODIPY and pyrene are coupled for Py$_2$D. Furthermore, the individual absorption bands are broadened compared with those of the other compounds, with a half-width of about 1000 cm^{-1}, which might indicate variable degrees of π conjugation for the ground-state species.

Fluorescence is readily observed for Py$_2$D in MTHF at room temperature, this being fully supported by excitation spectra, with the emission maximum being located at 727 nm (Figure 7). This corresponds to the relatively large
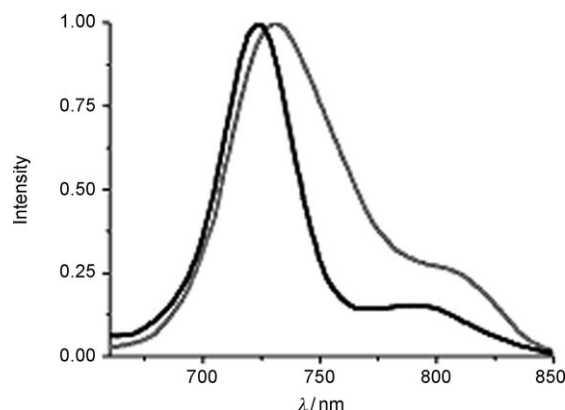

Figure 7. Fluorescence spectra recorded for Py$_2$D in MTHF at room temperature (grey curve) and 77 K (black curve).

Stokes' shift of 660 cm^{-1}. The Φ_F remains reasonably high, given the low energy of the emission maximum,[22] and the lifetime is comparable to those recorded for the other derivatives. As found throughout this work, both medium- and low-frequency vibrations are coupled to deactivation of the excited state and the derived $h\omega_M$ term remains closely comparable to those found for the other derivatives. At room temperature, the corresponding $h\omega_L$ is slightly smaller than those found for the ethenyl and styryl compounds. There is, however, a marked increase in S_Δ for Py$_2$D relative to the other derivatives that must arise from the different type of connection at the BODIPY unit. On cooling to 77 K, the emission spectrum narrows and becomes better resolved (Figure 7). The fluorescence maximum shifts to 723 nm, representing a blue shift of 40 cm^{-1}, in contrast to the compounds described above for which the glassy matrix favours a red shift. At 77 K, S_Δ decreases substantially to 0.20 while the individual peaks become slightly narrower ($\Delta\nu_{1/2} = 685$ cm^{-1}); note that the impression of a narrower emission profile at 77 K is caused by the change in S_Δ rather than $\Delta\nu_{1/2}$. Both $h\omega_M$ ($=1030$ cm^{-1}) and $h\omega_L$ ($=435$ cm^{-1}) decrease at 77 K relative to room temperature, but there is no splitting, as observed above. As such, there are important differences in the behaviour of the ethynylene derivatives relative to the other families.

Comparison of the bis-pyrenyl derivatives: The optical properties recorded for these extended BODIPY dyes are fully consistent with strong electronic interactions between the peripheral aryl polycycle(s) and the central BODIPY core. To compare the efficiencies of the various spacer groups in promoting this interaction, we now compare the properties of the three bis-pyrenyl compounds, namely Py_2B, Py_2C and Py_2D, measured in MTHF. As a starting point, we contrast the relevant absorption spectral profiles (Figure 8). It can be
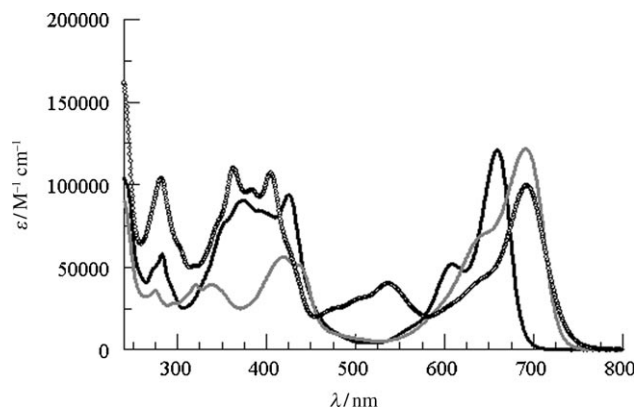

Figure 8. Comparison of absorption spectra recorded for Py_2B (black), Py_2C (grey) and Py_2D (open circles) in MTHF.

seen that, whereas Py_2B exhibits what might be considered to be a conventional spectrum with limited coupling between the subunits, the spectra recorded for both Py_2C and Py_2D show some unusual features. The lowest-energy transition, being closely associated with the BODIPY chromophore, is red-shifted and broadened, although ε_{MAX} remains similar in each case. For Py_2B, the lowest-energy pyrene-based absorption band appears as a series of sharp peaks between 430 and 320 nm, which arises from two or more overlapping transitions. For Py_2C, these individual transitions are split into two well-resolved sets of bands centred at 430 and 340 nm, respectively. More significant perturbations are seen for Py_2D, for which the pyrene-based chromophore exhibits a set of absorption transitions in the region from 550 to 440 nm, in addition to a stronger series of optical bands appearing between 420 and 320 nm. This splitting, and the inversion of the intensity levels, of the pyrene-based absorption bands ensures that Py_2D is an effective photon collector over much of the visible range.

The fluorescence spectra confirm the reduced HOMO–LUMO energy gaps for Py_2C and Py_2D relative to Py_2B and show the relative broadening of the bands for the former compounds (Figure 9). The pronounced spectral broadening apparent for Py_2D is a consequence of the significant contribution made by $\hbar\omega_L$. Indeed, for this latter compound it is noticeable that $\hbar\omega_L$ takes on a particularly small value. Most of the other derived properties (Tables 2 and 4) remain comparable for the various compounds, except for S_Δ, which is much higher for Py_2D. This latter finding can be attributed to the ethynylene group being more strongly coupled to the
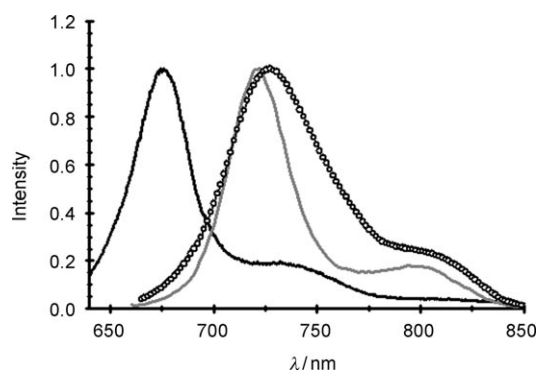

Figure 9. Comparison of fluorescence spectra recorded for Py_2B (black), Py_2C (grey) and Py_2D (open circles) in MTHF at room temperature. The spectral profiles are insensitive to changes in excitation wavelength.

BODIPY unit than is found for an ethenylene group. The k_{RAD} values are set by the confines of the Strickler–Berg expression,[23] but variations in k_{NR} are more difficult to explain. This term increases slightly on going from Py_2B ($k_{NR} = 5.1 \times 10^7$ s^{-1}) to Py_2C ($k_{NR} = 5.8 \times 10^7$ s^{-1}), despite the fall in the HOMO–LUMO energy gap, but undergoes a threefold increase on going to Py_2D ($k_{NR} = 15.3 \times 10^7$ s^{-1}). On cooling to 77 K, Py_2D shows a blue-shifted emission spectrum, in contrast to the red shifts observed for both Py_2B and Py_2C. Furthermore, the glassy matrix has the effect of splitting the accompanying vibronic modes for Py_2B and Py_2C but not for Py_2D. Again, Py_2D shows a reduced S_Δ at 77 K in contrast to all the other compounds. Thus, the ethyne linker behaves differently to its ethene counterpart.

An exception to the rule—Ant_2C: The ethenylene-bridged bis-anthracene derivative, Ant_2C, is insoluble in nonpolar solvents, but dissolves slowly in MTHF to give a blue-coloured solution. The resultant absorption spectrum is quite unlike those recorded for the other derivatives and consists of a broad, featureless transition centred at 632 nm (Figure 10). A similar spectrum is observed in dibutyl ether (Bu_2O), this being the least polar solvent that dissolves the compound. Spectral deconvolution indicates that the absorption transition is best described in terms of a progression of three Gaussian-shaped bands of common half-width (full
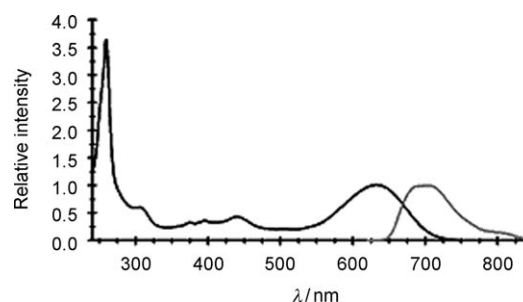

Figure 10. Absorption (black curve) and fluorescence (grey curve) spectra recorded for Ant_2C in dibutyl ether.

width at half maximum (FWHM) = 1855 cm^{-1}). Notably, the half-width greatly exceeds those measured for any other compound studied here. The maximum of the lowest-energy Gaussian band lies at 15 630 cm^{-1} in MTHF, and is only slightly dependent on the nature of the solvent, at least in weakly polar media. The absorption band has the general appearance of a charge-transfer transition. In Bu$_2$O, weak fluorescence can be observed from Ant$_2$C at ambient temperature, with a broad maximum centred at 698 nm (Figure 10). Under these conditions, Φ_F was found to be 0.075, although spectral deconvolution is consistent with a series of relatively broad Gaussian bands (Table 4). Similar, but weaker, emission is observed in MTHF ($\lambda_{FLU} = 715$ nm), whereas the fluorescence becomes increasingly weaker and red-shifted as the polarity of the solvent is increased. The emission, like the corresponding absorption profile, is best described as being of charge-transfer character. The fluorescence lifetime measured in MTHF is 0.35 ns, where Φ_F is 0.038 (Table 3).

Temperature-dependent fluorescence studies were performed on Ant$_2$C in butyronitrile (BuCN). At room temperature, the weak emission ($\Phi_F = 0.025$) is centred at 722 nm, but this shifts to the red upon cooling. Thus, between 298 and 180 K, the emission maximum moves progressively towards 728 nm, while there is a threefold increase in Φ_F. The red shift can be attributed to the temperature-induced increase in the static dielectric constant of BuCN, whereas the increased intensity points to an activated decay route. As the solvent begins to freeze, there is an abrupt shift towards the blue region and a pronounced increase in the emission intensity. During this transformation, the fluorescence profile acquires the features expected for a BODIPY-based dye, with the maximum appearing at 710 nm for the dye within the glassy matrix. Excitation spectra recorded over the same temperature range confirm that the charge-transfer band, evident at ambient temperature, firstly moves slightly towards the red and then begins to evolve into a regular BODIPY-like transition as the solvent starts to freeze. The charge-transfer character is switched off in the glassy matrix, no doubt because of the rigidity and nonpolar environment, and normal BODIPY behaviour prevails. The excitation and emission maxima are consistent with those recorded for the other compounds in a glassy matrix.

The impression here is that Ant$_2$C acts as an intramolecular charge-transfer system, in marked contrast to the other dyes, for which π,π* interactions dominate. The charge-transfer character is lost at 77 K in a glassy matrix because of the sharp decrease in local polarity. Support for this assertion is provided by consideration of the cyclic voltammogram recorded for Ant$_2$C in CH$_2$Cl$_2$ (Figure 11). Thus, two peaks are seen upon reductive scans. The first reduction wave is quasi-reversible and corresponds to a one-electron half-wave potential of −1.33 V versus Fc/Fc$^+$ (where Fc refers to ferrocene). This process is attributed to the addition of one electron to the BODIPY nucleus. The second step, having a peak at −2.03 V versus Fc/Fc$^+$, is irreversible and is attributed to the addition of one electron to an an-
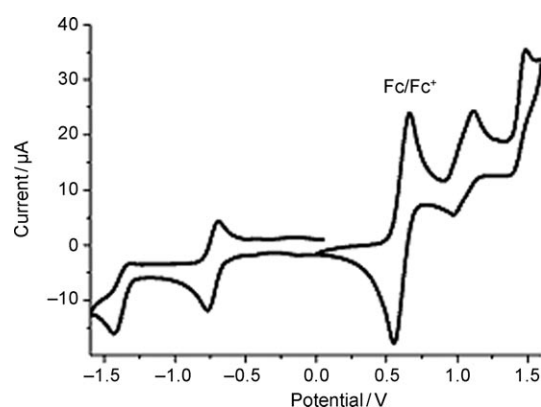

Figure 11. Cyclic voltammogram recorded for Ant$_2$C in CH$_2$Cl$_2$ containing background electrolyte and at a scan rate on 100 mVs^{-1}.

thracene moiety. Since this process is clearly a one-electron step, it follows that reduction of the second anthracene unit is suppressed, presumably because of electronic coupling along the molecular axis. The first oxidative wave corresponds to two overlapping peaks, each due to addition of one electron. The overall process is poorly reversible. The two half-wave potentials, derived from curve-fitting of the entire peak, are 0.42 and 0.47 V versus Fc/Fc$^+$. We attribute this process to the successive oxidation of each anthracene residue, with the splitting of 50 mV being taken as evidence for long-range electron delocalisation along the molecular backbone. There is a further two-electron oxidation peak centred at 0.89 V versus Fc/Fc$^+$, which is assigned to oxidation of the BODIPY core.

This interpretation of the cyclic voltammogram is consistent with the observation of intramolecular charge-transfer interactions in polar media. The situation, however, differs from that observed for other BODIPY–anthracene molecular dyads[11] built around conventional BODIPY units. Here, the two chromophores remain in electronic isolation but display fast intramolecular energy transfer. This is a clear indication of the effectiveness of the ethenylene linkage in providing electronic coupling between the residues.

Conclusion

These highly conjugated, BODIPY-type dyes operate as quasi-one-dimensional electronic systems, in which extended delocalisation of the π-electron backbone serves to decrease the HOMO–LUMO energy gap. There is a corresponding modification of the oscillator strength for the BODIPY-based transition found at low energy and of the position and shape of transitions associated with the appended aryl polycycle. Only the BODIPY-based, lowest-energy excited state emits and the radiative rate constant is fully consistent with the Strickler–Berg expression.[22] This relationship takes no direct account of the nature of the chromophore or of the conjugation length. However, the nonradiative rate constant might be expected to be more sensitive to structural changes

connected with the effective conjugation length. The latter is not easily established, especially for compounds of the type described here, despite its obvious importance for conducting polymers.[30] Recently, a rudimentary definition of the effective conjugation length (A_π) made use of Equation (1), in which β is an unspecified constant taken to equal unity.[31] Although there is a smooth evolution of Φ_F with the A_π value computed from Equation (1), this is not a useful definition of the effective conjugation length for molecular systems. Indeed, there is no global correlation between A_π and, for example, the emission maximum, although the data derived for the B series do show a smooth evolution. There is the additional problem that k_{RAD} increases with decreasing ν_{FLU}, as expected, but only within a given series of compounds. On the other hand, the corresponding nonradiative rate constant, k_{NR}, shows no obvious correlation with either ν_{FLU} or A_π. The impression, therefore, is that each series must be treated separately.

$$\frac{k_{RAD}}{k_{NR}} = e^{\beta A_\pi} \tag{1}$$

It is instructive at this point to compare the photophysical properties recorded for this series of fused BODIPYs with those measured for related BODIPY dyes in which the polycycle is attached to the boron centre, PyBPy.[20] In this latter case, the two units remain in electronic isolation and varying the size of the hydrocarbon has no effect on the optical properties of the BODIPY unit. Rapid electronic energy transfer occurs from the polycycle to the BODIPY core,[9] but the fluorescence lifetime and quantum yield of the BODIPY fluorophore are unperturbed by the nature of the substituent, provided that an appropriate solvent is used. On this basis, we can identify the boron linkage as being a poor electronic mediator. It is also known[2,6] that attaching the polycycle at the *meso* position does not perturb the photophysical properties of the BODIPY dye PymB, in part because the 1,7-methyl groups enforce a near-perpendicular arrangement of the BODIPY plane and the *meso*-aryl residue. It is only when the connection is made via conjugated groups at the 3,5-linkage that such effects are observed.

Finally, some comment is justified with regard to the fact that Ant$_2$C behaves differently to the other compounds studied here. It appears that charge-transfer effects out-

weigh the generic tendency to extend the π-electron conjugation length if suitable electron-donating and -withdrawing substituents are present. This behaviour introduces difficulties for compound design and also raises the possibility that dark charge-transfer states might contribute to the overall photophysical properties at slightly elevated temperatures. The situation is further complicated by the realisation that BODIPY can function as both an electron acceptor and donor with appropriate complementary reagents. Thus, charge-transfer effects have to be taken into account before designing the molecular structure. Despite this complication, it is now possible to identify putative BODIPY dyes for use in the far-red and near-IR regions that will be highly fluorescent. The most extreme example of this behaviour, at least from the new compounds reported here, concerns Pe$_2$B. This compound fluoresces at 755 nm with a quantum yield of 0.8 and a fluorescence lifetime of 3.6 ns. It does not aggregate in solution and looks to be a highly attractive addition to the BODIPY family. No fluorescence can be detected from the perylene units and the BODIPY-like S$_1$ state is formed within 0.35 ps after excitation into the perylene chromophore. It is likely that the emission wavelength could be pushed further towards the near-IR region by extending the conjugation or omitting the bridging phenylene rings.

Experimental Section

A full description of the synthesis and characterisation of all new compounds is given as part of the Supporting Information. Methyltetrahydrofuran was purchased as spectroscopic grade from Aldrich Chemicals Co.; it was used as received and found to be free from fluorescent impurities. Absorption spectra were measured with a Hitachi U3310 spectrophotometer and fluorescence spectra were measured with a fully corrected Jobin–Yvon Fluorolog tau-3 spectrofluorimeter. Fluorescence measurements were made using optically dilute solutions having an absorbance less than or equal to 0.05 at the excitation wavelength. Fluorescence quantum yields were measured relative to cresyl violet in methanol, taking due account of concentration effects, and were corrected for changes in refractive index. Lifetime measurements were made with a PTI EasyLife spectrometer using Ludox in distilled water to determine the instrumental response function to be used for subsequent deconvolution. Fluorescence was isolated with a high radiance monochromator after passing through suitable cut-off filters. The resolution of this instrument was approximately 150 ps after deconvolution. Further improvement in temporal resolution was achieved using a high-intensity, ultrashort laser diode as excitation source and a cooled Hamamatsu R3809U-50 photodetector in conjunction with a Becker and Hickl HFAC-26–01 pre-amplifier, applying time-correlated, single-photon counting methods. This set-up provided a wide range of excitation wavelengths and reduced the temporal resolution to about 30 ps. Low-temperature studies were performed with an Oxford Instruments Optistat DN cryostat; all solutions were purged with dried nitrogen before undertaking the measurements. Molar absorption coefficients were determined by weighing small samples of solid material using a micro-balance. At least three separate measurements were made in each case. Oscillator strengths and radiative lifetimes were calculated from signal-averaged spectral data.
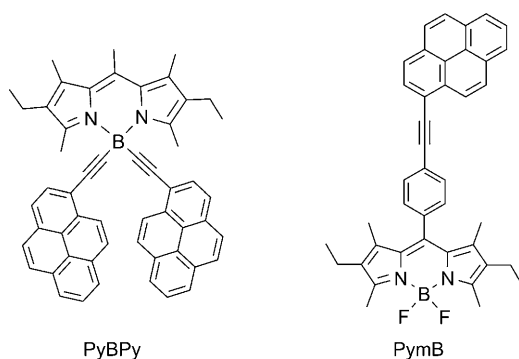
PyBPy

PymB

FULL PAPER

[1] J. R. Lakowicz, *Principles of Fluorescence Spectroscopy*, 3rd ed., Springer, Heidelberg, **2006**.

[2] a) A. Loudet, K. Burgess, *Chem. Rev.* **2007**, *107*, 4891–4932; b) R. Ziessel, G. Ulrich, A. Harriman, *New J. Chem.* **2007**, *31*, 7838–7851; c) R. Ziessel, *C. R. Acad. Sci. Chim.* **2007**, *10*, 622–642; d) G. Ulrich, R. Ziessel, A. Harriman, *Angew. Chem.* **2008**, *120*, 1202–1219; *Angew. Chem. Int. Ed.* **2008**, *47*, 1184–1201.

[3] a) R. P. Haughland, H. C. Kang, US Patent, US4774339, **1988**; b) H. C. Kang, R. P. Haughland, US Patent 5187288, **1993**; c) L. R. Morgan, J. H. Boyer, US Patent 5446157, **1993**; d) H. C. Kang, R. P. Haughland, US Patent 5451663, **1993**; e) H. C. Kang, R. P. Haughland, US Patent 5433896, **1995**; Y. Wu, D. H. Klaubert, H. C. Kang, Y.-Z. Zhang, US Patent 6005113, **1999**; f) E. Carreira, W. Zhao, PCT Patent WO 2006/058448, **2006**; g) G. Ulrich, C. Goze, R. Ziessel, PCT WO 2006/087459A2, **2006**; h) G. Ulrich, C. Goze, S. Goeb, A. De Nicola, R. Ziessel, PCT WO 2006/087458A2, **2006**.

[4] a) Z. Dost, S. Atilgan, E. U. Akkaya, *Tetrahedron* **2006**, *62*, 8484–8488; b) S. Atilgan, Z. Ekmekci, A. L. Dogan, D. Guc, E. U. Akkaya, *Chem. Commun.* **2006**, 4398–4400; c) A. Coskun, E. U. Akkaya, *J. Am. Chem. Soc.* **2006**, *128*, 14474–14475.

[5] a) A. Harriman, L. J. Mallon, K. J. Elliot, A. Haefele, G. Ulrich, R. Ziessel, *J. Am. Chem. Soc.* **2009**, *131*, 13375–13386; b) S. Diring, F. Puntoriero, F. Nastasi, S. Campagna, R. Ziessel, *J. Am. Chem. Soc.* **2009**, *131*, 6108–6110.

[6] R. Ziessel, C. Goze, G. Ulrich, M. Cesario, P. Retailleau, A. Harriman, J. P. Rostron, *Chem. Eur. J.* **2005**, *11*, 7366–7378.

[7] G. Ulrich, C. Goze, M. Guardigli, A. Roda, R. Ziessel, *Angew. Chem.* **2005**, *117*, 3760–3764; *Angew. Chem. Int. Ed.* **2005**, *44*, 3694–3698.

[8] A. A. Earp, G. B. Smith, P. D. Swift, J. Franklin, *Sol. Energy* **2004**, *76*, 655–667.

[9] a) A. Harriman, L. J. Mallon, S. Goeb, G. Ulrich, R. Ziessel, *Chem. Eur. J.* **2009**, *15*, 4553–4564; b) A. Harriman, L. J. Mallon, R. Ziessel, *Chem. Eur. J.* **2008**, *14*, 11461–11473.

[10] T. Rohand, W. Qin, N. Boens, W. Dehaen, *Eur. J. Org. Chem.* **2006**, 4658–4663.

[11] a) C.-W. Wan, A. Burghart, J. Chen, F. Bergström, L. B.-Å. Johansson, M. F. Wolford, T. GyumKim , M. R. Topp, R. M. Hochstrasser, K. Burgess, *Chem. Eur. J.* **2003**, *9*, 4430–4441; b) G.-S. Jiao, L. H. Thoresen, T. G. Kim, W. C. Haaland, F. Gao, M. R. Topp, R. M. Hochstrasser, M. L. Metzker, K. Burgess, *Chem. Eur. J.* **2006**, *12*, 7816–7826.

[12] M. Inouye, Y. Hyodo, H. Nakazumi, *J. Org. Chem.* **1999**, *64*, 2704–2710.

[13] M. Hissler, A. Harriman, A. Khatyr, R. Ziessel, *Chem. Eur. J.* **1999**, *5*, 3366–3381.

[14] H. Günther, in *NMR-Spektroskopie 3/E*, Thieme, Stuttgart, **1992**.

[15] E. Knoevenagel, *Ber. Dtsch. Chem. Ges.* **1898**, *31*, 2596–2619.

[16] a) M. Baruah, W. Qin, R. A. L. Vallée, D. Beljonne, T. Rohand, W. Dehaen, N. Boens, *Org. Lett.* **2005**, *7*, 4377–4380; b) T. Rohand, M. Baruah, W. Qin, N. Boens, W. Dehaen, *Chem. Commun.* **2006**, 266–268.

[17] a) L. Li, J. Han, B. Nguyen, K. Burgess, *J. Org. Chem.* **2008**, *73*, 1963; b) L. Li, B. Nguyen, K. Burgess, *Bioorg. Med. Chem. Lett.* **2008**, *18*, 3112; c) S. Rihn, P. Retailleau, N. Bugsaliewicz, A. De Nicola, *Tetrahedron Lett.* **2009**, *50*, 7008–7013.

[18] V. Leen, E. Braeken, K. Luckermans, C. Jackers, M. Van der Auweraer, N. Boens, W. Dehaen, *Chem. Commun.* **2009**, 4515–4517.

[19] W. W. Qin, T. F. Rohand, W. Dehaen, J. N. Clifford, K. Driessen, D. Beljonne, B. Van Averbeke, M. Van der Auweraer, N. Boens, *J. Phys. Chem. A* **2007**, *111*, 8588–8597.

[20] A. Harriman, G. Izzet, R. Ziessel, *J. Am. Chem. Soc.* **2006**, *128*, 10868–10875.

[21] W. W. Qin, M. Baruah, M. Van der Auweraer, F. C. De Schryver, N. Boens, *J. Phys. Chem. A* **2005**, *109*, 7371–7384.

[22] M. Bixon, J. Jortner, J. W. Verhoeven, *J. Am. Chem. Soc.* **1994**, *116*, 7349–7355.

[23] S. J. Strickler, R. A. Berg, *J. Chem. Phys.* **1962**, *37*, 814–822.

[24] R. Englman, J. Jortner, *Mol. Phys.* **1970**, *18*, 145–162.

[25] a) D. T. Piece, W. E. Geiger, *Inorg. Chem.* **1994**, *33*, 373–381; b) F. A. C. Oliveira, L. A. Cury, A. Righi, R. L. Moreira, P. S. S. Guimaraes, F. M. Matinaga, M. A. Pimenta, R. A. Nogueira, *J. Chem. Phys.* **2003**, *119*, 9777–9782.

[26] N. H. Damrauer, T. R. Boussie, M. Devenny, J. K. McClusker, *J. Am. Chem. Soc.* **1997**, *119*, 8253–8268.

[27] R. Croce, G. Zucchelli, F. M. Garlaschi, R. C. Jennings, *Biochemistry* **1998**, *37*, 17355–17360.

[28] A. Beeby, K. S. Findlay, A. E. Goeta, L. Porres, S. R. Rutter, A. L. Thompson, *Photochem. Photobiol. Sci.* **2007**, *6*, 982–986.

[29] R. Bonnett, A. Harriman, A. N. Kozyrev, *J. Chem. Soc. Faraday Trans.* **1992**, *88*, 763–780.

[30] L. T. Liu, D. Yaron, M. A. Berg, *J. Phys. Chem. C* **2007**, *111*, 5770–5782.

[31] Y. Yamaguchi, Y. Matsubara, T. Ochi, T. Wakamiya, Z.-I. Yoshida, *J. Am. Chem. Soc.* **2008**, *130*, 13867–13869.